Bachelor Project

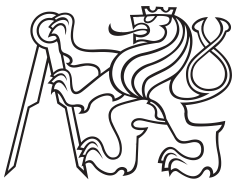

Czech Technical University in Prague

F3

Faculty of Electrical Engineering
Department of Cybernetics

Learning peripersonal space representations using spiking neural networks

Jiří Štěpanovský

Supervisor: Mgr. Matěj Hoffmann, Ph.D.
Supervisor–specialist: Ing. Zdeněk Straka
Field of study: Cybernetics and Robotics
May 2019

Acknowledgements

I would like to express my special thanks of gratitude to my supervisors for the opportunity to work on this thesis and for their golden patience during the final hours of writing, and also to my family and friends, who either directly or indirectly helped me bring this work into being.

Declaration

I declare that the presented work was developed independently and that I have listed all sources of information used within it in accordance with the methodical instructions for observing the ethical principles in the preparation of university theses.

Prague, 24. May 2019

Abstract

To guide the movement of the body through space, the brain must analyze the relation of the body position to nearby objects. This spacial awareness requires an integration of multiple sensory inputs and internal representation of the immediate surroundings, i.e., the peripersonal space.

We've implemented a biologically inspired computational model of peripersonal space representation using spiking neural network in the Neurorobotics platform and explored its dynamical properties during multiple learning scenarios. Finally, we've demonstrated the use of this model as a defense mechanism on an iCub robot in a simulated environment.

Keywords: Peripersonal space, spiking neural networks, receptive fields, synaptic learning mechanism

Supervisor: Mgr. Matěj Hoffmann, Ph.D.
Fakulta elektrotechnická,
Karlovo náměstí 13,
Praha 2

Abstrakt

Pro správnou orientaci pohybu těla v prostoru musí mozek neustále analyzovat pozici svého těla vůči poloze blízkých předmětů. Toto povědomí o okolním prostoru vyžaduje neustálé sjednocování senzorických podnětů z několika smyslů a tvorbu interní reprezentace peripersonálního prostoru.

V Neurorobotické platformě jsme implementovali biologicky inspirovaný model reprezentace peripersonálního prostoru pomocí "spiking" neuronových sítí a prozkoumali jsme jeho dynamické vlastnosti při ruzných typech učení. Nakonec jsme demonstrovali využití tohoto modelu k vyvolání obranné reakce na iCub robotu v simulovaném prostředí.

Klíčová slova: Peripersonální prostor, "spiking" neuronové sítě, receptivní pole, mechanismus synaptického učení

Překlad názvu: Učení se reprezentací peripersonálního prostoru pomocí "spiking" neuronových sítí

Contents

Figures

Tables

Chapter 1

Introduction

Automated systems and robots are becoming an indispensable component of modern industry and are replacing human counterparts in precise and repetitive operations. And by replacing many others it is increasing it's worth every day with other, more complex tasks. Even though most current designs are operating from a safe distance, the benefits of mutual interaction between human and robot workers are appealing. Unfortunately, progress is accompanied by tragic accidents [5]. Researchers from The National Institute for Occupational Safety and Health in the United States already identified 61 robot-related deaths just between 1992 and 2015 [9], and although from an analyzed set of accidents some are reportedly caused by human error [24], safety is still a big concern and a topic of great interest.

One of the fields of research trying not only to tackle the problem of human-robot interaction, but the interaction of robots with the environment in general, is the study of peripersonal space (PPS). Based on recent research in neuroscience [7], primate brains seem to construct multiple representations of space, collectively called PPS, which provide essential information to guide their body through space, avoid collisions, grasp objects and interact with immediate surroundings. These are the exact properties, that could help robots, which are today usually simplified just to their kinematic chains, to achieve more natural and more importantly safer movement through their dynamically changing environments in which they operate. If successfully applied, these robots are able to perceive their surroundings and avoid any hazardous situations, could significantly speed up the integration of robotics in spaces already occupied by people, making the research of PPS an important area to explore.

The circuitry in the brain specialized in representing space immediately surrounding the body was firstly explored in studies on macaque monkeys [26], [29], and later elaborated by Rizzolatti et al. [32], [31], who introduced the term PPS. By studying afferent properties of individual neurons, these papers describe a set of neurons, found predominantly caudal to the arcuate sulcus of macaques in the area F4, that are bimodal, responding to both visual and somatosensory stimuli. The visual receptive field of either bimodal neuron never exceeds the animal's reaching distance and is spatially related to the tactile receptive field of the same neuron; furthermore, both receptive fields are neither orientation nor direction selective. The bimodal neurons itself also do not code space in a coordinate system centered on the retina, rather, they use a coordinate system centered on a specific body part (i.e., hand-centered, head-centered, and trunk-centered) [2], [12]. Interestingly, their visual point of interest is not based solely on the current field of vision, but by utilization of working memory, once the animal is aware of a stimulus, corresponding bimodal neurons respond even if the stimulus is no longer in sight [15].

Since the underlying mechanisms of PPS and its emergence remains yet to be explained, together with direct neurological research, computational models are offering a more detailed view and inching us towards a comprehensive understanding. In this thesis, we present one such model based on existing work of Elisa Magosso et al. [28] implemented using spiking neural networks in the environment of the Neurorobotics Platform [1]. We focus on multiple stimulation scenarios and explore the effects such stimulations induce. Finally, we demonstrate the use of this model as a defense mechanism on an iCub robot in a closed-loop simulated environment.

Chapter 2

Related Work

2.1 Peripersonal space

Several areas have been found in the macaque brain to encode a multisensory map of space in a body part-centered frame of reference including the putamen, area F4, area 7b, and the Ventral Intraparietal Area [14]. These areas, illustrated in Figure 2.1, contain neurons with relatively large tactile receptive fields (RFs), located primarily on the face, neck, arms, hands, and face. Neurons are arranged in such a way to form a crude map of the body part surface, similarly to a cortical homunculus. A large portion of these neurons is bimodal, responding to both tactile and visual stimuli. The location of visual RFs is spatially related to the tactile RFs and never exceeds the animal's reaching distance. Therefore the bimodal neurons represent somatotopically organized space near the body.

Unlike classical visual neurons, bimodal neurons in these areas respond poorly to plain light stimuli far from the animal, but are most sensitive to real three-dimensional objects looming towards the body [32]. The maximal distance of these visual RFs varies from less than 10 cm to the farthest reachable area, but never exceeds it. However, the specific boundary is not hardcoded in the brain and can be altered, for example, through tool use. Another relevant characteristic of the visual RFs is that they are independent of eye movements [11]. Their location is always anchored to the tactile RFs of the body part, regardless of the body posture or visual fixation field of view, creating a body part-centered reference frame.

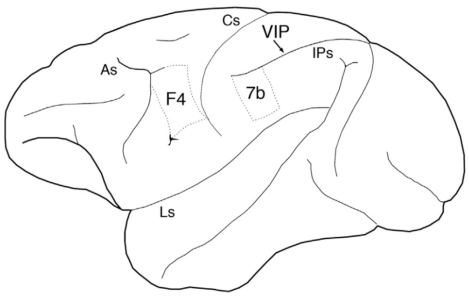

Figure 2.1: Lateral view of the monkey cerebral cortex showing three regions containing neuronal populations that selectively encode peripersonal space: area F4 in the frontal lobe, area 7b and the Ventral Intraparietal Area, which is buried in the depth of the intraparietal sulcus (IPs), in the parietal lobe. As=arcuate sulcus; Cs=central sulcus; Ls=lateral sulcus. Figure and caption from [7].

Multiple other findings are crucial in PPS representations. One of them being, that some bimodal neurons in area F4 exhibit the property of "object permanence" [15]. These neurons keep firing even after the initially presented and visible stimulus was silently (in the dark) removed. Such cells are thus utilizing working memory and higher cortical processes, and are not dependent on visual and tactile purely feed-forward stimuli. As such, the PPS representation can play a role in general movement through the environment even in the dark or in the direction outside of the field of vision.

Recordings of bimodal neurons in area F4 shows directional and proximity selectivity, but no change in response to a differently sized stimulus [16]. The results suggest that most bimodal cells are sensitive to the direction of motion of the stimulus, and although a wide range of directions is present, many neurons preferred looming stimuli. All these properties are represented in Figure 2.2, in which both directional and proximity selectivity resulted in higher cell activity, whereas differently sized stimulus had no effect.

Some bimodal neurons were shown to respond to visual stimuli presented near a fake stuffed monkey arm placed in a realistic posture [13] and that the visual RF was modulated by the movement of the fake arm. Furthermore, even when the real arm was moved out of view and only proprioceptive signals were available, the shift in the location of the visual RF was still present, suggesting the brain uses a convergence of visual and proprioceptive cues to determine the location of the body part.

Finally, it has been shown that neurons in the area F4 integrate not only tactile and visual stimuli, but also auditory stimuli within the corresponding PPS [17], creating a sensory complete representation of the space around the body.

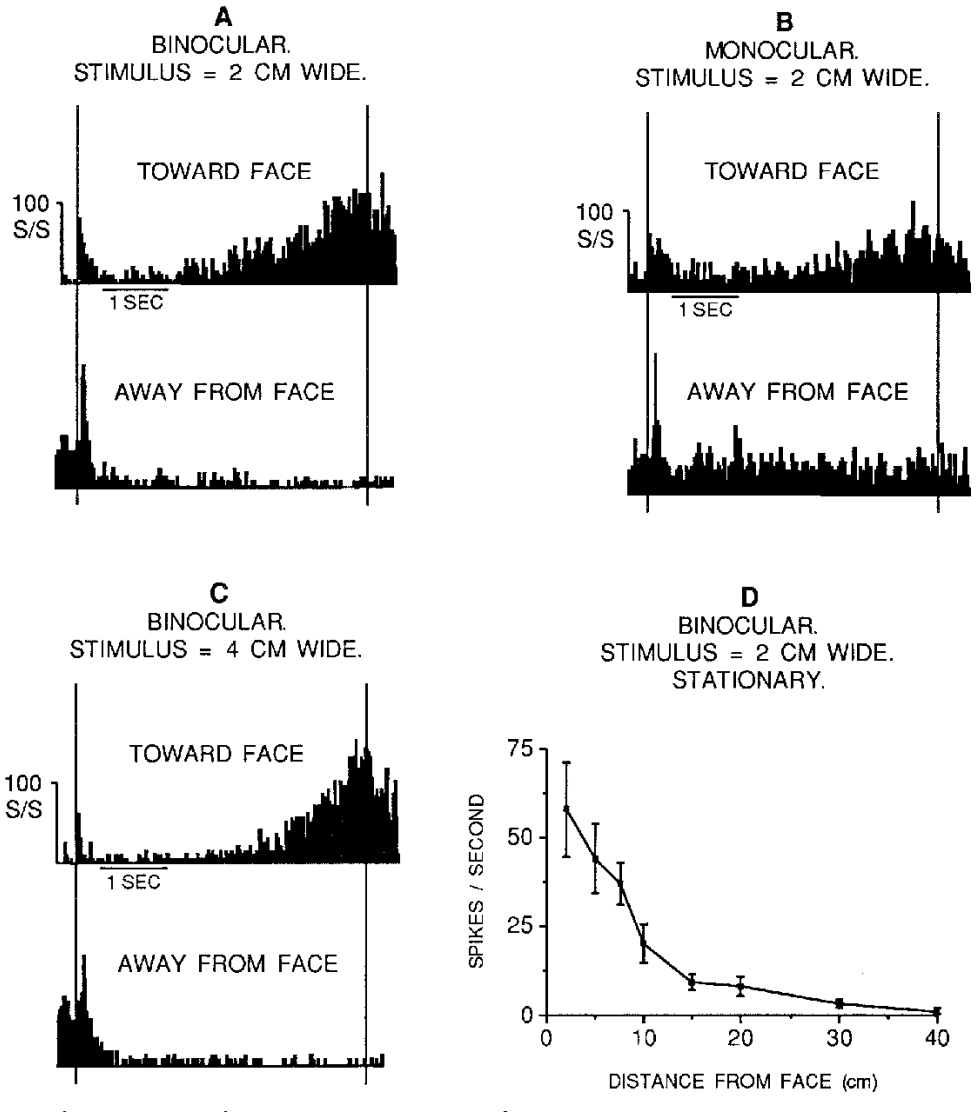

Figure 2.2: Responses of a bimodal neuron from premotor cortex with a tactile receptive field on the eyebrows. Each histogram is based on 10 trials. Stimuli were presented while the monkey was not performing the fixation task. In A–C the visual stimulus was advanced toward the face from in front at 8.25 cm/s and retracted on alternate trials. Stimulus farpoint = 37.5 cm, nearpoint = 2 cm, intertrial interval = 10 s. Vertical lines: onset and offset of stimulus movement. In A, the stimulus was a 2 x 2 cm square of cardboard viewed binocularly. The cell responded better as the stimulus approached. In B, one eye was covered, but the cell was still sensitive to depth. The baseline activity increased because the eye cover touched the tactile receptive field. In C, the stimulus was a 4 x 4 cm square of cardboard viewed binocularly. The increase in stimulus size did not cause a corresponding increase in response. In D, stationary stimuli were tested at eight different distances. The cell still preferred nearby stimuli, even though all motion cues for depth had been eliminated. Figure and caption from [16].

2.2 Peripersonal space development and plasticity

Human infants seem to be born without any notion of PPS, as they are not able to reach, grasp, or in any other way interact with the environment around them, and their motions are seemingly aimless. But throughout an unguided experience, they learn to contact nearby objects and later to grasp them with a reasonable degree of reliability [3], and with successive training, their initially jerky and uncertain movements become increasingly refined.

A behavior closely attributed to the development of PPS is a spontaneous self-touching by human infants in the first six months [35]. The behavior is believed to be an important developmental phase that allows the coordination of reaching and grasping motions. It is also supported by an experiment, suggesting, that at early stages the development of PPS seems to be dependent purely on proprioceptive cues [6], as the success rate of an object grasping by young infants is unaffected when the hand is not visible. The vision then becomes increasingly important toward the end of the first year for smooth movements and anticipation of contact with an object.

It is thought that the PPS remains dynamic and adaptable to the environment throughout the whole life. One of the main experiment demonstrating this property is based on the fascinating idea that tools become extensions of our body [23], [4], [8]. Results collectively show that during and a couple of minutes after the tool use the visual RFs of bimodal neurons are altered and enlarged to include the effective length of the tool. While it is generally accepted that these results serve as evidence for PPS adaptation, there are interpretations explaining the results in a different view [19] or dismissing the hypothesis of PPS extension altogether [20], [18]. Nonetheless, the underlying mechanisms of the visual RFs alternations during tool use are still debated and far from understood.

2.3 Computational models

Numerous computational models, often supported by neurophysiological experiments, are trying to explain and simulate some of the attributes of PPS. One such model proposed by Magosso et al. [28] is focusing precisely on the previously mentioned plasticity through tool-use. Assuming that the modification of peri-hand space arises from a Hebbian growing of visual synapses, while other synapses remain unmodified, the model consisted of two

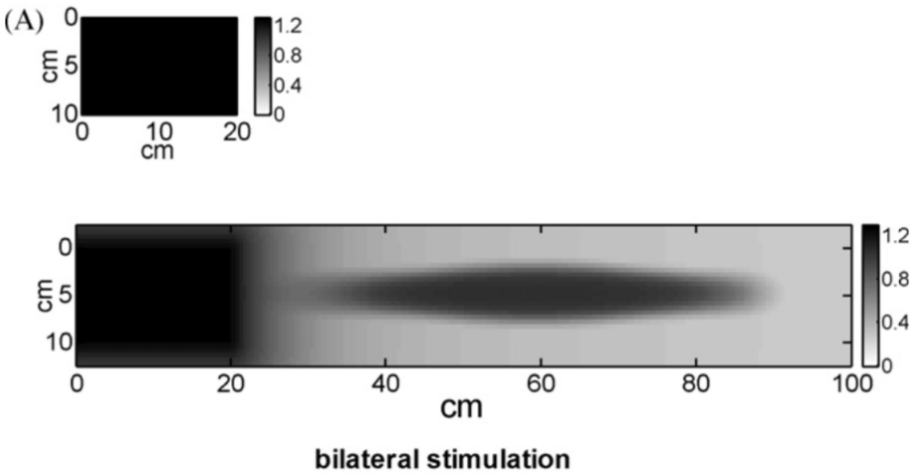

Figure 2.3: Feedforward synapses from unimodal layers to a single multimodal neuron. Visual synapses reinforce to integrate the tip of the tool in the PPS. Figure and caption adopted from [28].

mutually inhibiting hemispheres, each having only the visual feed-forward connection plastic. It predicted a PPS extension after tool use, independently of whether the tool was present or absent in the hand of the subject at the time (Figure 2.3). The results had been validated by an in-vivo experiment on a right brain-damaged patient suffering from visual-tactile extinction, providing strong evidence for the plausibility of the model.

A different approach, yet, based on the same neural network architecture, by Jean-Paul Noel et al. [30] is exploring the PPS from the position of dynamical, i.e., instantaneous, adaptation as opposed to long-lasting changes. As mentioned above, the PPS depth is changing as a function of the velocity of incoming stimuli. They propose an audio-tactile model implementing a neural adaptation to persistent stimulation as a mechanism interpreting this phenomenon. Again, supported by behavioral observations, the model can effectively differentiate between various stimuli speeds, as illustrated in Figure 2.4.

Furthermore, studies more directly focused on robotics are exploring the use of PPS representations in an object manipulating or object avoidance tasks. A biologically motivated model by Roncone et al. [33] implemented on a humanoid robot is able to learn its PPS representation through the real-time interaction with humans and can be utilized in behaviors like avoidance and reaching. Likewise, a model developed by Straka and Hoffmann [34] is excelling in the ability to predict the position of potential impact with an approaching object.

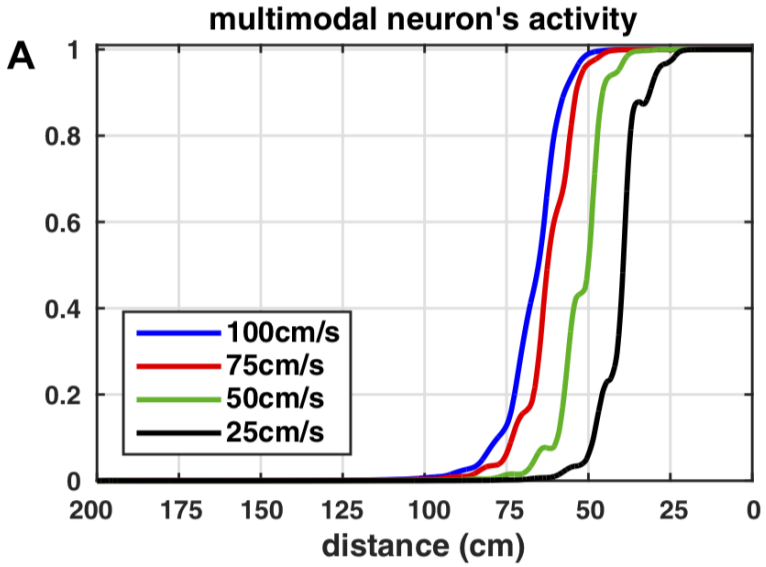

Figure 2.4: Response of the multisensory neuron in the peri-face space network to a sound given alone, moving at four different velocities, as a function of the sound distance from the face. Figure and caption adopted from [30].

Other, closely similar computational models exist, although not necessarily related to PPS representations. However, one model by Osamu Hoshino [21] deserves mention, since, unlike any other previously described model of sensory integration, it is the only one proposing a direct connection between unisensory areas, not just a link between them through the multisensory layer. Due to this connection, the model is able to produce a faster response to a cross-modal stimulus, than relying purely on the top-down influence of multisensory populations.

In the next chapter, we introduce the platform we've worked with and use the work mentioned above in order to develop our own model of PPS.

Chapter 3

Materials and Methods

3.1 Neurorobotics platform

A robot mind interacting through its body with the environment around makes an important closed loop system, which gives rise to an aim-oriented behavior. This perception-action loop is an emerging point of interest for neuroscience and robotics, both united under the field of neurorobotics. One of the leading projects is Neurorobotics Platform (NRP) under the development of the European Union-funded Human Brain Project [25].

NRP is simplifying the development of our PPS models by providing a bridge between Gazebo [10] physics engine running a simulation of a robot body and environment, and a spiking neural network simulator NEST [22] running the robot's brain. The communication between the two is provided by transfer functions (TFs), written in python, which are called synchronously in discrete time intervals, set to $T_{TF} = 20ms$. This time interval is necessary to take into account and is the cause of discretization as evident in the result below.

The main function of TFs is to gather all the necessary data from the physics engine, like value from a sensor, position of an object or an image from a simulated camera, and "transfer" them into the neural network in two ways. Either as a spike train or a source injecting a current into one or many neurons. In the same manner, they are also responsible for data extraction from the neural network and controlling the robot actuators according to

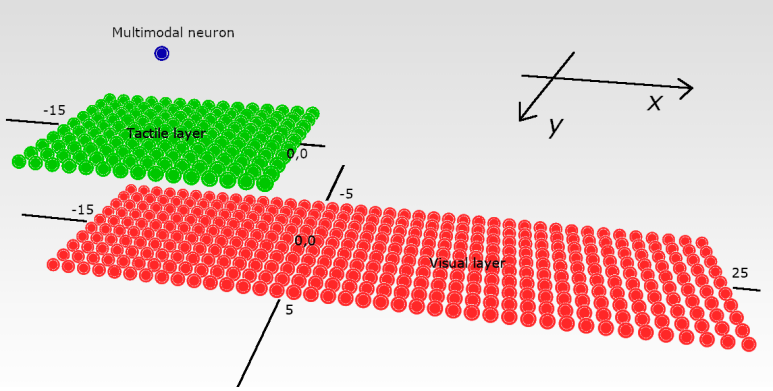

Figure 3.1: The architecture of our model's neural network. A single multimodal neuron is integrating information from visual and tactile sensory inputs.

them. TFs are therefore closing the loop between a robot's brain and the simulated robot body and environment.

Most of our experiments do not utilize the physics engine and are based solely on a neural network and a couple of TFs managing the stimulation of the neural network. The physics engine is used only in the last experiment, where an application of the modeled PPS is used as a proof-of-concept experiment demonstrating a simple defense mechanism.

3.2 Neural model

Architecture of our neural network model is inspired by the state of the art computational model, as of now, able to cover several PPS properties including somatotopic organization, cross-modal extinction and facilitation [27], expansion upon tool-use [28] and dynamic resizing [30], even though, not all of them at the same time. Although the model is based on a neural network, the neurons in question are modeled as a first-order dynamical system with sigmoidal, and therefore continuous, output function. Such model of neurons is not easily compatible with an integrate and fire neurons available in the NRP, and therefore some parameters, namely the weights, had to be altered.

As illustrated in Figure 3.1, the network's architecture consists of one multimodal neuron integrating information from two sensory modalities – tactile, representing the somatosensory input of the robot, and visual, representing the robot's sight. Both modalities consist of somatotopically arranged neurons, stimulated by direct sensory input. The model corresponds

to an immobile robot with a square body of size $M^t \times N^t$ cm covered with skin, operating in a two-dimensional environment, having visual information about the entire area of its body and a space in front of it for a total size of $M^v \times N^v$ cm.

All neurons in the network are leaky integrate and fire models with fixed threshold and alpha-function shaped post-synaptic current (in NRP labeled as "IF_curr_alpha"). Both tactile and visual layers are connected with the multimodal neuron through feedforward and feedback connections but aren't connected between themselves. If no stimulation to input layers is applied, the network is quiet, and no activity is present, and while the network itself is run in the NEST simulator, the stimulation has to be artificially injected through TF.

The skin, covering the robot's body, is represented by a tactile neural layer of size $M^t \times N^t$ neurons, where each neuron has its RF defined as a two-dimensional Gaussian function $\Phi^t_{ij}(x, y)$:

$$\Phi^t_{ij}(x,y) = \Phi^t_0 \cdot exp\Big(- \frac{(x - x^t_{ij})^2 + (y - y^t_{ij})^2}{2 \cdot (\sigma^t)^2}\Big),$$

where the center of the RF (x^t_{ij}, y^t_{ij}) is defined for each tactile neuron ij as:

$$(x^t_{ij}, y^t_{ij}) = (j - M^t + 0.5, i - N^t/2 + 0.5)\ cm \quad j = 1, 2, ..., M^t \ \ i = 1, 2, ..., N^t.$$

The robot's vision is, again, represented by a neural layer, where each visual neuron has RF with a center (x^v_{ij}, y^v_{ij}) defined by a function:

$$\Phi^v_{ij}(x,y) = \Phi^v_0 \cdot exp\Big(- \frac{(x - x^v_{ij})^2 + (y - y^v_{ij})^2}{2 \cdot (\sigma^v)^2}\Big),$$

$$(x^v_{ij}, y^v_{ij}) = (j - M^t + 0.5, i - N^t/2 + 0.5)cm \quad j = 1, 2, ..., M^v \ \ i = 1, 2, ..., N^v.$$

By using these positions, all visual neurons with RF in the negative plane of X-axis are representing a stimulus within the robot's body, while the ones with RF in the positive plane of X-axis are representing a stimulus in front of the body.

The input to both unimodal layers is a stimulus at a position (x^s, y^s), with an amplitude defined by a function:

$$S(x,y) = S_0 \cdot exp\Big(- \frac{(x - x^s)^2 + (y - y^s)^2}{2 \cdot (\sigma^s)^2}\Big),$$

so the total input current φ_{ij} (uA) into each unimodal neuron is a sum of the stimulus amplitude and the neuron's RF:

$$\varphi_{ij}^{m} = \sum_{x}\sum_{y} \Phi_{ij}^{m}(x,y) \cdot S(x,y) \qquad m = t, v$$

Computed input currents are injected into the network using TF, and therefore, the update frequency is limited by the NRP's update time T_{TF}. Hence, the movement of a stimulus is only approximated by updating its position each time the TF is called:

$$(x_{t+1}^{s}, y_{t+1}^{s}) = (x_{t}^{s}, y_{t}^{s}) + T_{TF} \cdot (v_{x}^{s}, v_{y}^{s}).$$

The network is interconnected via several synaptic connections. Static lateral synapses connect neurons within unimodal layers, static feedback synapses project from multimodal neuron to unimodal layers, and feedforward synapses carry stimulation data from unimodal layers up to the multimodal neuron.

The static lateral synapses within an unimodal layer have a "mexican hat" shaped excitation. An actively firing neuron is therefore exciting other neurons in close proximity, while inhibiting the ones far away. The function determining the synaptic weight between two neurons ij and kl in the same modality is:

$$\Lambda_{ij,kl} = \Lambda_0^P \cdot exp\Big(-\frac{(x_{ij}-x_{kl})^2 + (y_{ij}-y_{kl})^2}{2\cdot(\sigma^P)^2}\Big) - \Lambda_0^N \cdot exp\Big(-\frac{(x_{ij}-x_{kl})^2 + (y_{ij}-y_{kl})^2}{2\cdot(\sigma^N)^2}\Big).$$

The static feedback synapses from the multimodal neuron to every neuron in both tactile and visual layers have all the same weight of B. Similarly, all feedforward synapses from each neuron in the tactile layer to the multimodal neuron have the weight of W.

The feedforward synapses from visual layer to multimodal neuron, on the other hand, are plastic, using the default spike-timing-dependent plasticity (STDP) mechanism provided by the NEST simulator. The weights are limited to a maximum value of Q_{max} and the default values for an ij neuron in the visual layer are initialized as followed:

$$Q_{ij} = \begin{cases} Q_0 & j \leq M^t \\ 0 & j > M^t \end{cases}$$

All constants mentioned above are stated in table 3.1.

Name	Label	Value
TF update time (ms)	T_{TF}	20
Size of the tactile layer along X-axis	M^t	15
Size of the tactile layer along Y-axis	N^t	10
Size of the visual layer along X-axis	M^v	40
Size of the visual layer along Y-axis	N^v	10
Strength of the tactile RF	Φ_0^t	1.5
Strength of the visual RF	Φ_0^v	1.5
Deviation of the tactile RF	σ^t	1.0
Deviation of the visual RF	σ^v	1.0
Strength of the stimulus	S_0	4.0
Deviation of the stimulus	σ^s	1.5
Positive amplitude of lateral "mexican hat" synapses	Λ_0^P	2.7
Negative amplitude of lateral "mexican hat" synapses	Λ_0^N	2.0
Positive deviation of lateral "mexican hat" synapses	σ^P	2.0
Negative deviation of lateral "mexican hat" synapses	σ^N	4.5
Weight of feedback synapses	B	0.4
Weight of tactile feedforward synapses	W	1.0
Maximum weight of visual STDP synapses	Q_{max}	1.0
Default weight of visual STDP synapses	Q_0	0.8

Table 3.1: Constants used in the neural network model of PPS.

3.3 iCub PPS model

To demonstrate a practical use case of our model, a fully-featured closed-loop system was implemented in the NRP. The architecture of the model remains mostly the same, though, the dimensions are modified. In contrast to the previously described model, this one utilizes the Gazebo physics engine to actually simulate the robot's body and generate the sensory inputs. Finally, by connecting an actuator to the multimodal neuron, the model is able to generate behavior.

The whole setup can be seen in Figure 3.2, an iCub robot in the simulated environment was placed in such a posture to look downwards. A stimulus, represented by a red ball, is looming towards the robot's torso, while his right arm is raised to a position, where it does not intersect the ball's trajectory but is able to if the shoulder is yawed.

The tactile layer is reduced to a single neuron and therefore no lateral synapses are present. To account for the reduction in quantity, the feedforward synapse weight W is increased. The input current of the tactile neuron is

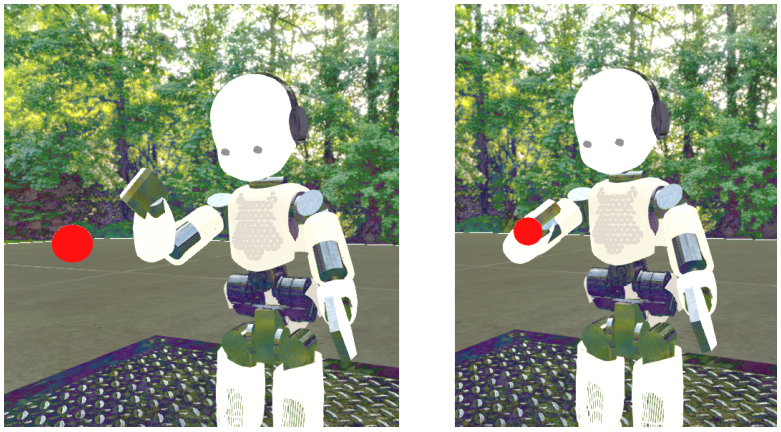

Figure 3.2: The setup of an iCub robot in the simulation. Left: Right arm in a default position does not intersect the red ball's trajectory. Right: If yawed, the right arm is in the way between the red ball and the robot's torso.

Name	Label	Value
Size of both visual layers	V	10
Weight of the tactile feedforward synapse	W	10.0
Input current into tactile neuron upon collision	S_0^t	10.0

Table 3.2: Constants used in the iCub neural model.

dependent on the collision test of robot's torso with other objects, and can be defined as:

$$\varphi^t = \begin{cases} S_0^t & \textit{collision detected} \\ 0 & \textit{otherwise} \end{cases}$$

So once the looming ball contacts the torso, the tactile neuron becomes active.

The visual layer is now split into two layers of size $V \times V$, one layer for each eye. The current inputs of the visual neurons are computed separately for the left and right eye and are defined by a function:

$$\varphi_{ij}^v = 0.008 \cdot \frac{R_{ij}}{G_{ij} \cdot B_{ij}} \qquad i, j = 1, 2, ..., V,$$

where R_{ij}, G_{ij}, B_{ij} are direct values of red, green and blue color of a pixel from an image captured by an eye at position ij.

The last addition to this model is the ability to interact with its environment. The positioning of the right arm is directly proportional to the activity of the multimodal neuron, and as a result, stimulation of the neural network causes the right arm to yaw and intersect the trajectory of the red ball.

Chapter 4

Results

4.1 Receding stimulus

The First experiment, performed on the PPS model with single bimodal cell, demonstrates the effect of receding stimuli. One learning iteration consisted of a stimulus moving at a constant speed along the X-axis away from the body from coordinates (-17, 0) to (27, 0). Both the starting and ending position of the stimulus were outside of the visual RF bounds, so the outer positions of the stimulus had no impact on the learned representation. Three different stimulus speeds were tested: 7.5, 15, and 30 cm/s.

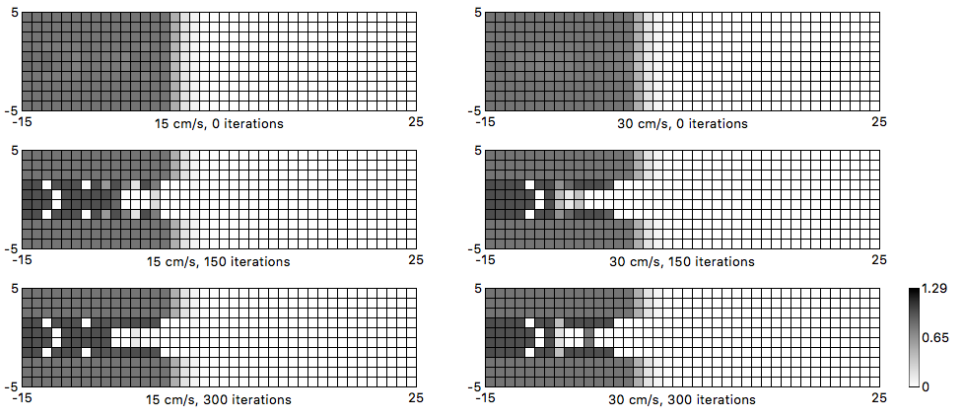

Figure 4.1: Weights of visual feedforward synapses after 150 and 300 iterations of stimuli receding away from the body at a constant speed of 15 cm/s (left) and 30 cm/s (right).

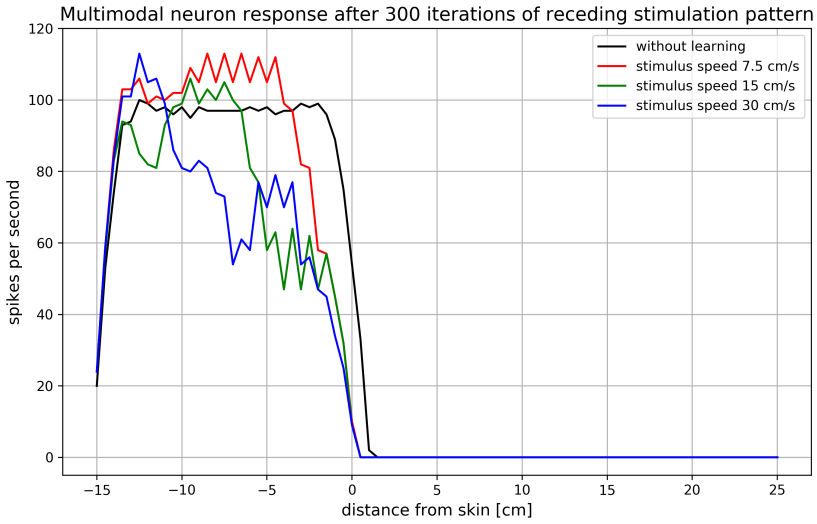

Figure 4.2: Multimodal neuron activity to a stimulus applied throughout the X-axis of the input layers RF after 300 iterations of receding stimuli.

The weights of visual feedforward synapses, modified after 300 iterations by the STDP algorithm, can be seen in Figure 4.1. The visual RF have reduced in size and, as a consequence, multimodal neuron exhibited a weaker activity near the edge of the body, compared to the reasonably even response before the stimulation, Figure 4.2. The speed of receding stimuli appears to have an influence on the margin, by which the PPS representation reduces, since, the faster the stimulation was, the stronger the attenuation of the multimodal neuron activity at the body boundary has become.

4.2 Looming stimulus

An opposite scenario was produced by reversing the direction of the stimulus. Once the stimuli were looming towards the body, again, along the X-axis from coordinates (27, 0) to (-17, 0) at a constant speed of 15 cm/s, the visual RF has expanded, Figure 4.3, as opposed to the previous experiment.

Even though the stimulus was looming towards the body on one side, since it maintained its motion, it was actually receding from the body on the other. So naturally, we can see the same outcome of the RF contraction as in the previous experiment, only mirrored.

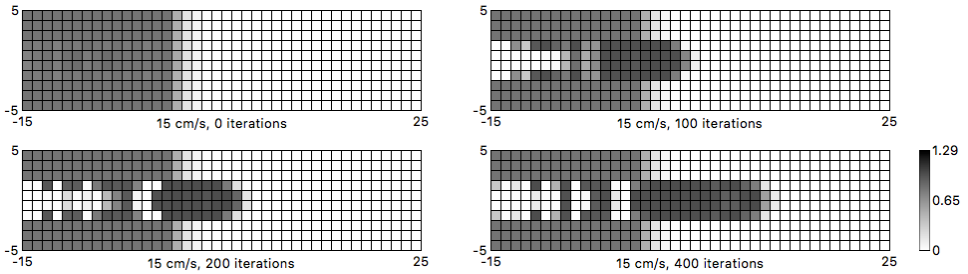

Figure 4.3: Weights of visual feedforward synapses during the learning of 400 iterations of a looming stimulus with a speed of 15 cm/s.

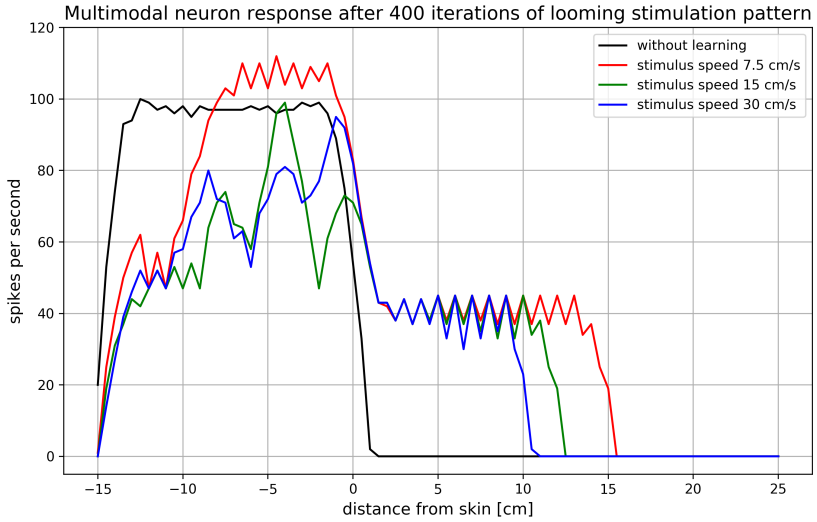

Figure 4.4: Multimodal neuron activity to a stimulus applied throughout the X-axis of the input layers RF after 400 iterations of looming stimuli.

By testing multiple speeds, we can confirm from Figure 4.4 that on the "receding" side of the body the visual RF has again reduced more with faster speeds. On the other hand, the "looming" side gives exactly opposite results. Here, the slowest speed had produced the biggest expansion of the RF, while the fastest stimulation produced the smallest effect. Also evident is the limited activity of the PPS representation to stimuli outside of the body's area, because of the absence of tactile sensory input.

Plotting the distance of the stimulus from the body, at which the multimodal neuron became active, we can estimate the PPS representation size throughout the stimulation. Testing the same speeds as previously, as illustrated in figure 4.5, it is even more visible that the slowest stimulation produced the largest expansion of the visual RF. Furthermore, the expansion rate seems to be linear and, as such, not limited by the distance from the actual body.

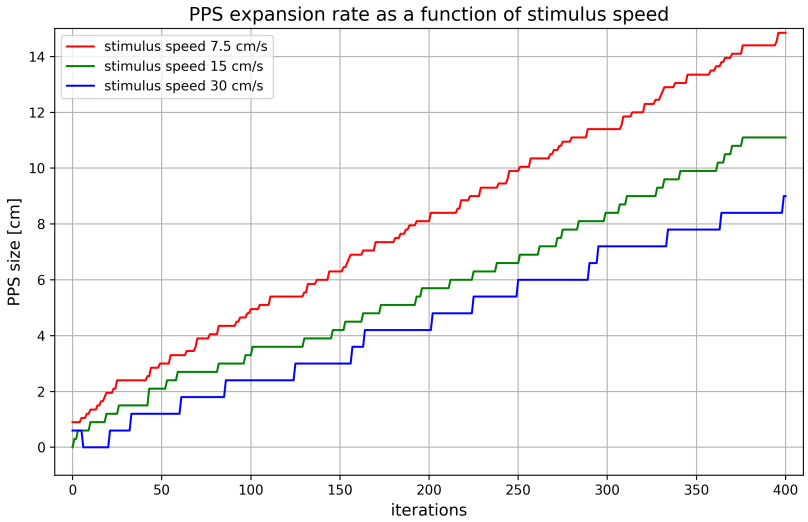

Figure 4.5: PPS expansion during looming stimuli of speeds 7.5, 15, and 30 cm/s.

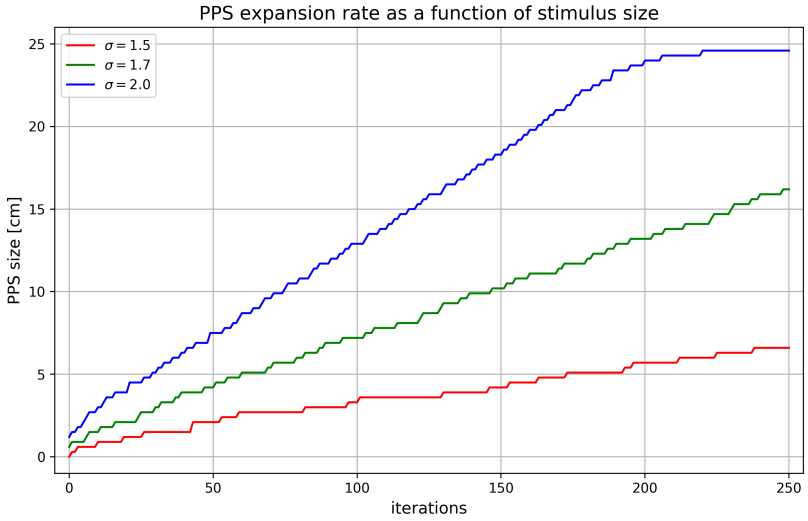

Figure 4.6: PPS expansion during looming stimuli of different sizes.

If we vary the size of the stimulus by changing the value of σ^s, Figure 4.6, we can see a more expected outcome, as the greater stimulus resulted in a faster expansion rate of the PPS representation. But again, the increase is linear and is limited only by the boundary of our model's visual input layer.

4.3 Looming and receding stimulus

All previous experiments suffer from a reduction of the visual RF inside the body. But by removing the discontinuity from the stimulation, so that the stimulus moves along the X-axis from coordinates (27, 0) to (-10, 0) and then back to (27, 0), this issue disappears, as seen in Figure 4.7. Even after 100 iterations, the response to stimulation throughout the entire surface of the body remained mostly unchanged, Figure 4.8. But the unnatural property that slower stimuli caused significantly faster expansion of the PPS still remains, Figure 4.9, and seems to be even greater, since the speed of 30 cm/s resulted in almost no expansion of the visual RF.

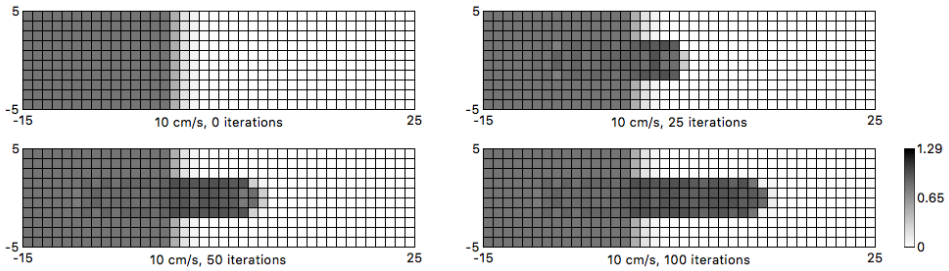

Figure 4.7: Weights of visual feedforward synapses during the learning through 100 iterations of looming and then receding stimuli with a speed of 10 cm/s.

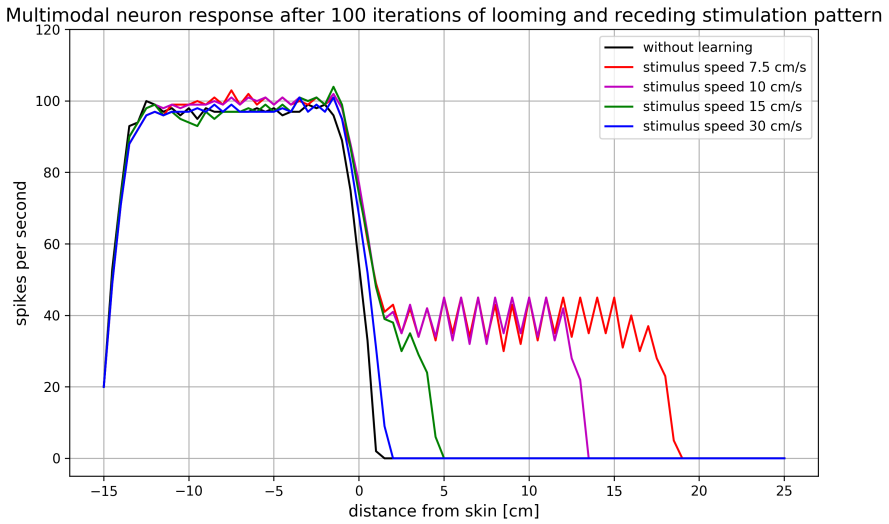

Figure 4.8: Multimodal neuron activity to a stimulus applied throughout the X-axis of the input layers RF after 100 iterations of looming and receding stimuli.

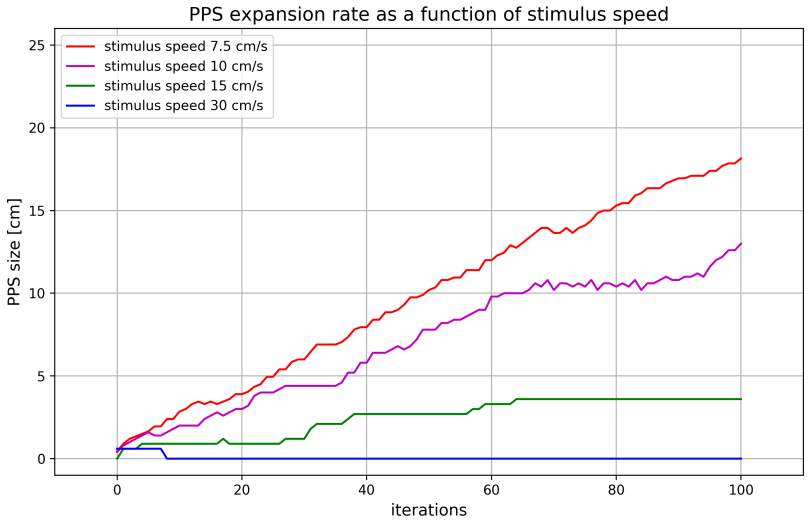

Figure 4.9: PPS expansion during looming and receding stimuli of speeds 7.5, 10, 15, and 30 cm/s.

4.4 iCub model

We have subjected the model to a looming stimulation. Each iteration consisted of a red ball moving from outside of the robot's field of vision towards the robot's chest at a speed of 50 cm/s. Upon collision with the robot, the stimulus was removed shortly after the tactile input neuron became activated.

The learned visual RFs after just a couple of iterations for left and right eyes are visualized in Figure 4.10. Expectedly, both RF has enlarged in the same manner as in previous experiments, with a looming stimulus. In this scenario, however, both sensory inputs were based on physics simulation, therefore, demonstrating the practical use of the model to represent external stimuli.

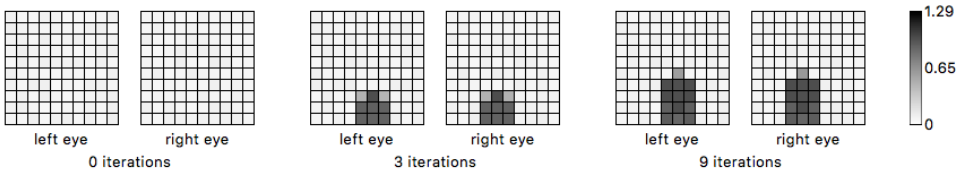

Figure 4.10: Weights of visual feedforward synapses during learning PPS representation with a stimulus of a speed 50 cm/s.

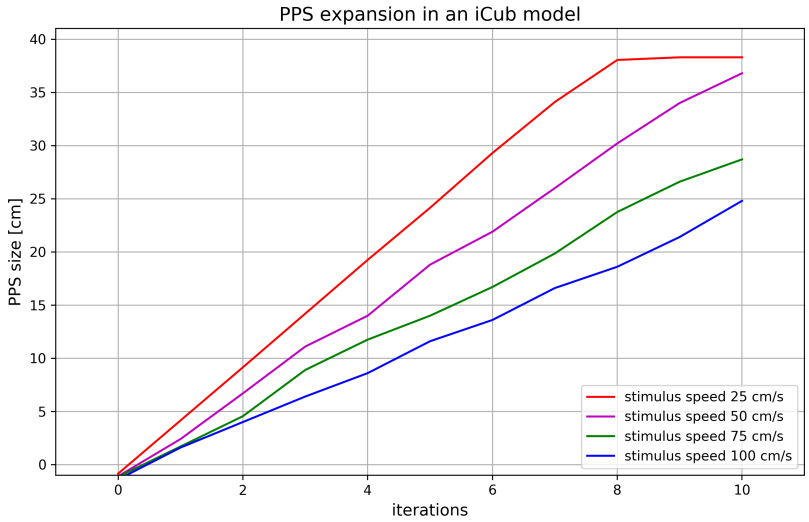

Figure 4.11: PPS expansion of an iCub model during looming stimuli of speeds 25, 50, 75, and 100 cm/s.

By varying the speed of the looming stimulus, in accordance with previous experiments, the slowest speed has again produced the most dominant change in PPS representation, as seen Figure 4.11. Because of the reduced size of the network, the extension rate in the simulated environment was faster compared to the previous experiments, but remains linear and unlimited.

The last and foremost important experiment performed with our spiking neural implementation of PPS in the closed-loop environment of NRP is the addition of an actuator connected to the multimodal neuron. Until now, the model was only a passive system implementing a crude version of unsupervised learning, but with the ability to intersect the red ball's path by stimulating the right arm, the model gains the ability to influence the place of collision.

As illustrated in Figure 4.12, where the Y-axis represents the distance of the red ball from the iCub robot, the model has been learning the PPS representation during the first stimulus iterations but in some cases, already 2 iterations the visual RF was strengthened enough, to induce a sufficient activity in the multimodal neuron to move with the iCub's arm and prevent the collision.

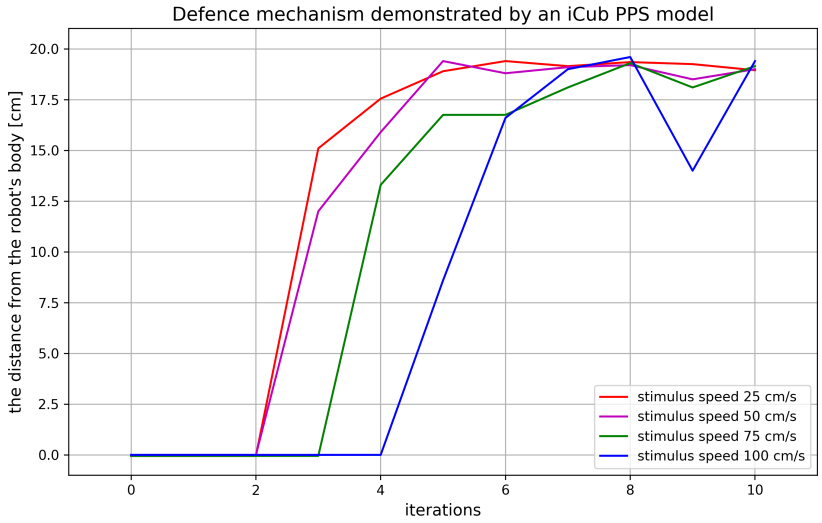

Figure 4.12: Distance of the red ball from the iCub robot upon collision.

Chapter 5

Conclusion and Discussion

We have implemented a biologically inspired computational model of peripersonal space representation using a spiking neural network in the Neurorobotics platform. The model integrates sensory input from visual and tactile modality and is able to adapt to dynamic stimulation.

Subjecting the network to a receding stimulation resulted in a reduction of the represented peripersonal space. Since there's not much information regarding this phenomenon, it is unclear, if the property could be assumed as evidence for or against the model's biological plausibility. Nevertheless, it seems very unlikely to consistently occur during usual interaction with the environment.

The expansion of the represented space upon approaching stimulus is, however, a property of great value, and can be most likely linked to the early development of the peripersonal space [3], [35] or as a general prediction mechanism [34]. Sadly, the achievement is undercut with the effect of self-sustained, unlimited expansion. Because it is evident that the real peripersonal space never exceeds the body's reaching distance, either the brain limits the boundary by yet another mechanism, or the means necessary for learning are not sufficiently complete.

Another property directly conflicting with the biological data is the strong influence of the stimulus size, which is not present in the biological counterparts [16]. It's hard to think of a solution to this problem, and while lateral synapses help in this regard, probably more layers are needed between the unimodal layer of the peripersonal model and the direct sensory input.

In short, while, our model can successfully integrate spatial information from multiple modalities and can be utilized in a prediction based tasks focusing on margin of safety around the robot, it seems unable to achieve any high-order characteristics such as direction selectivity, object permanence, selective attention, or a instantaneous adaptation based on stimulation speed [30].

Therefore, it is evident from the attributes of our model and from the current research, that more work is indeed required to build a coherent and potentially useful model of peripersonal space.

Appendix A

Bibliography

[1] *The neurorobotics platform*, The Human Brain Project (2015), Available at https://neurorobotics.net [accessed May 15, 2019].

[2] Richard A. Andersen, *Inferior parietal lobule function in spatial perception and visuomotor integration*, Behavioural Brain Research, 10.1002/cphy.cp010512 (2011).

[3] N. E. Berthier, *The syntax of human infant reaching*, Unifying Themes in Complex Systems: Proceedings of the 8th International Conference on Complex Systems, volume VIII of New England Complex Systems Institute Series on Complexity **8** (2011), 1477–1487.

[4] Anna Berti and Francesca Frassinetti, *When far becomes near: Remapping of space by tool use*, Journal of Cognitive Neuroscience **12** (2000), 415–420.

[5] B. Brumfield, *Car assembly line robot kills worker in germany*, CNN (2015), Available at http://www.cnn.com/2015/07/02/europe/germany–volkswagen–robot–kills–worker/ [accessed May 1, 2019].

[6] Rachel K. Clifton, Darwin W. Muir, Daniel H. Ashmead, and Marsha G. Clarkson, *Is visually guided reaching in early infancy a myth?*, Child Development **64** (1993), 1099–1110.

[7] Giuseppe di Pellegrino and Elisabetta Làdavas, *Peripersonal space in the brain*, Neuropsychologia **66** (2015), 126–133.

[8] Alessandro Farnè, Andrea Serino, and Elisabetta Làdavas, *Dynamic size-change of peri-hand space following tool-use: Determinants and spatial characteristics revealed through cross-modal extinction*, Cortex **43** (2007), no. 3, 436–443.

[9] The National Institute for Occupational Safety and Health, *Cdc - robotics: About the center - niosh*, Centers for Disease Control and Prevention (2017), Available at https://www.cdc.gov/niosh/topics/robotics/aboutthecenter.html [accessed May 2, 2019].

[10] Open Source Robotics Foundation, *Gazebo*, [Software], Available at http://gazebosim.org [accessed May 22, 2019].

[11] M. Gentilucci, C. Scandolara, I. N. Pigarev, and G. Rizzolatti, *Visual responses in the postarcuate cortex (area 6) of the monkey that are independent of eye position*, Experimental Brain Research **50** (1983), no. 2, 464–468.

[12] M. E. Goldberg, C. L. Colby, and J.-R. Duhamel, *Representation of visuomotor space in the parietal lobe of the monkey*, Cold Spring Harb Symp Quant **55** (1990), 729—-739.

[13] Michael S. A. Graziano, *Where is my arm? the relative role of vision and proprioception in the neuronal representation of limb position*, Proceedings of the National Academy of Sciences of the United States of America **96** (1999), 10418–10421.

[14] Michael S. A. Graziano and Charles G. Gross, *The representation of extrapersonal space: A possible role for bimodal, visual-tactile neurons*, The cognitive neurosciences (1995), 1021–1034.

[15] Michael S. A. Graziano, Xin Tian Hu, and Charles G. Gross, *Coding the locations of objects in the dark*, Science **277** (1997), 239–241.

[16] _____, *Visuospatial properties of ventral premotor cortex*, Journal of Neurophysiology **77** (1997), no. 5, 2268–2292.

[17] Michael S. A. Graziano, Lina A. J. Reiss, and Charles G. Gross, *A neuronal representation of the location of nearby sounds*, Nature **397** (1999), 420–430.

[18] Nicholas Holmes, *Does tool use extend peripersonal space? a review and re-analysis*, Experimental brain research **218** (2012), 273–282.

[19] Nicholas P. Holmes, Gemma A. Calvert, and Charles Spence, *Extending or projecting peripersonal space with tools? multisensory interactions highlight only the distal and proximal ends of tools*, Neuroscience Letters **372** (2004), 62–67.

[20] Nicholas P. Holmes, D. Sanabria, Gemma A. Calvert, and Charles Spence, *Tool-use: capturing multisensory spatial attention or extending multisensory peripersonal space?*, Cortex **43** (2007), no. 3, 469–489.

[21] Osamu Hoshino, *Neuronal responses below firing threshold for subthreshold cross-modal enhancement*, Neural Computation **23** (2011), 958–983.

[22] The NEST Initiative, *Gazebo*, [Software], Available at https://www.nest–simulator.org [accessed May 22, 2019].

[23] A Iriki, Michio Tanaka, and Yoshiaki Iwamura, *Coding of modified body schema during tool use by macaque postcentral neurones*, Neuroreport **7** (1996), 2325–2330.

[24] Bernard C. Jiang and Charles A. Gainer, *A cause-and-effect analysis of robot accidents*, Journal of Occupational Accidents **9** (1987), 27–45.

[25] Alois Knoll and Marc-Oliver Gewaltig, *Neurorobotics: A strategic pillar of the human brain project*, Science Robotics (2016).

[26] L. Leinonen and G. Nyman, *Ii. functional properties of cells in anterolateral part of area 7 associative face area of awake monkeys*, Experimental Brain Research **34** (1979), 321–333.

[27] Elisa Magosso, Andrea Serino, Melissa Zavaglia, Giuseppe di Pellegrino, and Mauro Ursino, *Visuotactile representation of peripersonal space: A neural network study*, Neural Computation **22** (2009), 190–243.

[28] Elisa Magosso, Mauro Ursino, Giuseppe di Pellegrino, Elisabetta Làdavas, and Andrea Serino, *Neural bases of peri-hand space plasticity through tool-use: Insights from a combined computational–experimental approach*, Neuropsychologia **48** (2010), 812–830.

[29] V. B. Mountcastle, *The world around us: Neural command functions for selective attention.*, Neurosciences Research Program Bulletin **14** (1976), 1–47.

[30] Jean-Paul Noel, Olaf Blanke, Elisa Magosso, and Andrea Serino, *Neural adaptation accounts for the dynamic resizing of peri-personal space: Evidence from a psychophysical-computational approach*, Journal of Neurophysiology **119** (2018), 2307–2333.

[31] Giacomo Rizzolatti, Cristiana Scandolara, Massimo Matelli, and Maurizio Gentiluci, *Afferent properties of periarcuate neurons in macaque monkeys. i. somatosensory responses*, Behavioural Brain Research **2** (1981), 125–146.

[32] ———, *Afferent properties of periarcuate neurons in macaque monkeys. ii. visual responses*, Behavioural Brain Research **2** (1981), 147–163.

[33] Alessandro Roncone, Matej Hoffmann, Ugo Pattacini, Luciano Fadiga, and Giorgio Metta, *Peripersonal space and margin of safety around the body: Learning visuo-tactile associations in a humanoid robot with artificial skin*, PLoS One **11** (2016), e0163713.

[34] Zdenek Straka and Matej Hoffmann, *Learning a peripersonal space representation as a visuo-tactile prediction task*, International Conference on Artificial Neural Networks. Springer, Cham (2017).

[35] Brittany L. Thomas, Jenni M. Karl, and Ian Q. Whishaw, *Independent development of the reach and the grasp in spontaneous self-touching by human infants in the first 6 months*, Frontiers in psychology **5** (2015), 1526.

Appendix B

CD content

The attached CD contains the following files:

- this document in as a pdf;
- folder with experiment files of receding stimulus;
- folder with experiment files of looming stimulus;
- folder with experiment files of looming and receding stimulus;
- folder with scripts for figures generation;
- a Readme file with instructions.

BACHELOR'S THESIS ASSIGNMENT

I. Personal and study details

Student's name: **Štěpanovský Jiří** Personal ID number: **466199**

Faculty / Institute: **Faculty of Electrical Engineering**

Department / Institute: **Department of Cybernetics**

Study program: **Cybernetics and Robotics**

II. Bachelor's thesis details

Bachelor's thesis title in English:

Learning Peripersonal Space Representations Using Spiking Neural Networks

Bachelor's thesis title in Czech:

Učení se reprezentací peripersonálního prostoru pomocí "spiking" neuronových sítí

Guidelines:

1. Study literature on peripersonal space (PPS) representations and computational models thereof.
2. Familiarization with Neurorobotics Platform (NRP, http://www.neurorobotics.net) and models of spiking neural networks.
3. Learning scenarios for PPS from simulated visual and tactile inputs.
4. Experimentation with different learning architectures and settings (unimodal and multimodal neural populations, Hebbian learning rules, Spike timing dependent plasticity).
5. Evaluation of learning speed and properties of learned representations with respect to input and network parameters. Basic comparison with PPS representations in primate brains (see Noel et al. 2018).
6. Exploration the possibility of extension of the model to iCub humanoid robot with sensitive skin and 3D environment model in NRP. Discussion of the possibility of using the representation as a module for safe human robot interaction.

Bibliography / sources:

[1] Magosso Elisa, et al. "Neural bases of peri-hand space plasticity through tool-use: Insights from a combined computational–experimental approach." Neuropsychologia 48.3 (2010): 812-830.
[2] Noel Jean-Paul, et al. "Neural adaptation accounts for the dynamic resizing of peripersonal space: evidence from a psychophysical-computational approach." Journal of neurophysiology 119.6 (2018): 2307-2333.
[3] Knoll Alois and Gewaltig Marc-Oliver. "Neurorobotics: a strategic pillar of the Human Brain Project." Science Robotics (2016).
[4] Roncone Alessandro, Hoffmann Matej et al. "Peripersonal space and margin of safety around the body: learning visuo-tactile associations in a humanoid robot with artificial skin." PloS ONE 11.10 (2016): e0163713.
[5] Straka Zdenek, Hoffmann Matej. "Learning a peripersonal space representation as a visuo-tactile prediction task." International Conference on Artificial Neural Networks. Springer, Cham, (2017).

Name and workplace of bachelor's thesis supervisor:

Mgr. Matěj Hoffmann, Ph.D., Vision for Robotics and Autonomous Systems, FEE

Name and workplace of second bachelor's thesis supervisor or consultant:

Ing. Zdeněk Straka, Vision for Robotics and Autonomous Systems, FEE

Date of bachelor's thesis assignment: **09.01.2019** Deadline for bachelor thesis submission: **24.05.2019**

Assignment valid until: **20.09.2020**

Mgr. Matěj Hoffmann, Ph.D.	doc. Ing. Tomáš Svoboda, Ph.D.	prof. Ing. Pavel Ripka, CSc.
Supervisor's signature	Head of department's signature	Dean's signature

III. Assignment receipt

The student acknowledges that the bachelor's thesis is an individual work. The student must produce his thesis without the assistance of others, with the exception of provided consultations. Within the bachelor's thesis, the author must state the names of consultants and include a list of references.

. _____
Date of assignment receipt

_____
Student's signature